CHARACTERIZATION AND CATALYTIC PERFORMANCE ON TRANSESTERIFICATION OF PALM OLEIN OF POTASSIUM OXIDE SUPPORTED ON RH-MCM-41 FROM RICE HUSK SILICA

Surachai Artkla[1], Nurak Grisdanurak[2], Suthasinee Neramittagapong[3], and Jatuporn Wittayakun[1*]

Abstract

A mesoporous material, RH-MCM-41, was synthesized with a rice husk silica source by hydrothermal method. The obtained material showed characteristic X-ray diffraction peaks of the (100), (110), and (200) planes at 2.3, 4.0 and 4.7 degrees, respectively, and possessed a high specific surface area of 1,231 m^2/g and narrow pore size distribution in the range of 1.8 - 4.2 nm. It was used as a catalytic support for potassium oxide (K_2O) from a CH_3COOK precursor to produce K_2O/RH-MCM-41 with K_2O loading of 4, 8, and 12%wt. Upon loading with K_2O, the RH-MCM-41 surface area decreased significantly indicating the collapse of the mesoporeous structure, and the tendency to collapse increased with the K_2O loading. The K_2O/RH-MCM-41 catalysts were tested for biodiesel production from palm olein oil and methanol via transesterification at 50, 75, and 100°C. The catalyst with 8% K_2O loading gave the highest conversion at all tested temperatures. At this loading, the activity increased with the temperature and the highest conversion was 84% at 100°C. Products from transesterification were mainly methyl palmitate (C16) and unsaturated methyl ester (oleate, linoleate and linolenate, C18).

Keywords: RH-MCM-41, MCM-41, K_2O, Transesterification, Biodiesel, Heterogeneous catalysis

Introduction

MCM-41, one of the M41S families has attracted wide interest because of its excellent properties such as large surface area (1,000-1,400 m^2/g), well defined regular pore diameter (20 - 100 Å), narrow pore size distribution, and thermal stability. Normally, MCM-41 can be synthesized by mixing a silica source such as sodium silicate, fumed silica, or tetraethylorthosilicate with a

[1] *School of Chemistry, Institute of Science, Suranaree University of Technology, Nakhon Ratchasima, 30000, Thailand. Tel.:0-4422-4256; Fax.: 0-4422-4185; Email: jatuporn@sut.ac.th*

[2] *Department of Chemical Engineering, Faculty of Engineering, Thammasat University, Pathumthani, 12120, Thailand.*

[3] *Department of Chemical Engineering, Faculty of Engineering, King Mongkut's Institute of Technology, Ladkrabang, Bangkok, 10520, Thailand.*

[*] *Corresponding author*

template solution and crystallized under hydro-thermal conditions (Bialek *et al.*, 1991; Kumar *et al.*, 2001). After separation of the solid crystals from the solution, the organic template can be removed by calcination at 540°C to result in MCM-41 (Grisdanurak *et al.*, 2003).

Because of its properties, MCM-41 can be used as a support for immobilization of metal catalysts. In this work, it was synthesized with rice husk silica, assigned as RH-MCM-41, and further used as a support for K_2O and the catalyst would be referred to as K_2O/RH-MCM-41. This catalyst was basic and suitable for catalysis that requires basicity such as transesterification. Thus, this research focused on the catalysis of K_2O/RH-MCM-41 for transesterification that converts triglyceride from oil/fat and alcohol to alkyl esters to produce glycerol and methyl ester or biodiesel (Eqn. 1).
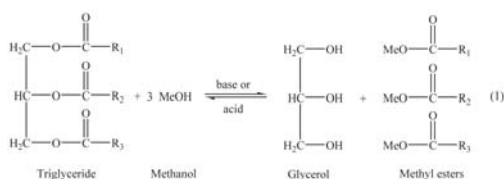
Conventionally, the homogeneous base catalysts such as NaOH, KOH, and $NaOCH_3$ are preferred because they produce high yields of the alkyl ester product, the reaction time is short (about 2 h), and the cost of raw materials is low. Unfortunately, the use of base catalysts is limited only to well-refined vegetable oil with less than 2.0% free fatty acid (FFA) in order to avoid the formation of soap, an undesired by-product. In addition, it is difficult to separate ester products from glycerol by-products in homogeneous catalysis and the yield of methyl esters is low (Ma and Hanna, 1999). Heterogeneous catalysis could overcome these drawbacks.

Here we report the preparation of RH-MCM-41 and K_2O/RH-MCM-41 and character-ization by X-ray diffraction (XRD) and the Brunauer-Emmett-Teller method (BET). The catalysis of K_2O/RH-MCM-41 for the biodiesel production was also studied to understand the effects of reaction temperature and potassium oxide content.

Experimental

Silica Extraction

Rice husk silica (RHS) was prepared by acid leaching and calcinations as described by Khemthong *et al.* (2007). The element analysis of white rice husk silica (RH-SiO$_2$) by X-ray fluorescence showed that the purity of silica was 98% along with trace amounts of alumina, potassium oxide, and calcium oxide. The XRD pattern of RH- SiO$_2$ exhibited a broad 2θ peak at 22° which is a characteristic of amorphous silica. Its specific surface area from the BET surface area analysis was 234.5 m^2/g.

Preparation of RH-MCM-41

RH-MCM-41 was synthesized by a proce-dure modified from literature (Srinivas *et al.*, 2004) with the gel molar ratio of $1.0SiO_2 : 3.0NaOH : 0.25CTABr : 180H_2O$. Briefly, cetyltrimethy-lammonium bromide (CTABr) and RH-SiO$_2$ (in 3.33M NaOH solution) were dissolved in distilled water and stirred for 4 h. The pH was adjusted to 11.5 by 5 N H_2SO_4 and the gel mixture was crystallized in a teflon-linen autoclave ands annealed hydrothermically in an oven at 100°C for 72 h. After filtration and drying at 100°C, the powder was washed with distilled water and calcined at 540°C to remove the template and characterized by XRD and BET.

Preparation of K_2O/RH-MCM-41

K_2O/RH-MCM-41 was prepared by the impregnation method adapted from literature with K_2O loading of 4, 8, and 12%wt (Xie *et al.*, 2006). The dried RH-MCM-41 was mixed with CH_3COOK in methanol solution and vigorously stirred for 3 h. Finally, the mixture was washed with distilled water, calcined at 500°C for 5 h and characterized by XRD and BET.

Characterization or RH-MCM-41 and K_2O/RH-MCM-41

Powder XRD patterns were obtained using Cu Kα radiation on a Bruker-AXS D5005 diffractometer (Bruker AXS GmbH, Karlsruhe, Germany) in which the samples were scanned from 2θ of 1.5 to 15.0 degree.

Nitrogen adsorption-desorption isotherms

were determined at -196°C from a relative pressure of 0.001 - 0.990 at the standard temperature and pressure (STP) on an ASAP 2010 analyzer (Micromeritics Instrument Corporation, Georgia, USA). Before measurement, each sample was degassed at 300°C for 12 h. The pore size and pore volumes were calculated from the desorption branches of the isotherm using the Barrett-Joyner-Halenda method (BJH).

Catalytic Testing for Transesterification

Triglyceride (palm olein oil) used as a raw material for reaction consisted of 39.8%wt. palmitic acid (C16:0), 54.0%wt. unsaturated acids [oleic acid (C18:1), linoleic acid (C18:2), and linolenic acid (C18:3)], and 4.4%wt. stearic acid (C18:0) (Department of Agriculture, 2007). Palm olein oil (4.0 cm^3) was preheated to reaction temperature and added to a mixture of methanol (10.0 cm^3) and catalyst (0.3 g). The mixture was stirred for 7 h at 50, 75, or 100°C. During the reaction, a pale yellowish liquid was formed and the viscosity of the mixture decreased significantly. The pale yellowish solution was evaporated to remove the excess methanol and the resulting liquid was separated from the catalyst by gravity under refrigeration. The obtained yellowish solution, which contained fatty acid methyl ester (FAME) was analyzed by a GC14-A gas chromatograph (Shimadzu Scientific Instrument, Kyoto, Japan) equipped with a flame ionization detector.

Results and Discussion

Characterization of RH-MCM-41 and K$_2$O/RH-MCM-41 by XRD and BET

The XRD patterns of RH-MCM-41 and K$_2$O/RH-MCM-41 with K$_2$O loading of 4, 8, and 12%wt. are shown in Figure 1. The spectrum of RH-MCM-41 showed the characteristic reflections of the (100), (110) and (200) planes of hexagonal structure at 2.3, 4.0, and 4.7 degrees, respectively, similar to that of MCM-41 from literature (Papp *et al*,. 2005). When RH-MCM-41 was loaded with potassium oxide, the only peak observed was that of the (100) plane and the intensity decreased with the amount of K$_2$O. This

indicated that the mesoporeous structure of RH-MCM-41 collapsed upon the K$_2$O addition. The position of the (100) peak also shifted to a higher value with the K$_2$O amount indicating the decrease of d-spacing. The position of the (100) peak, unit cell width (a*), and calculated d$_{100}$ are shown in Table 1. Thus, the K$_2$O loading affected the RH-MCM-41 hexagonal structure and the surface area of RH-MCM-41 was expected to decrease upon the K$_2$O loading. For 12%K$_2$O/ RH-MCM-41, the (100) peak was barely observable indicating that its mesoporeous structure collapsed almost completely. Although it was still unclear about the structure of the collapsed RH-MCM-41, the catalysis of 12%K$_2$O/RH-MCM-41 was investigated and compared with that of 12%K$_2$O/RH-SiO$_2$, which was less porous, to observe the influence of support.

The nitrogen adsorption-desorption isotherms of RH-MCM-41 and K$_2$O/RH-MCM-41s are displayed in Figure 2. RH-MCM-41 and 4%K$_2$O/RH-MCM-41 gave a Type-IV isotherm with three well-defined stages. In the first step, the adsorption at relative pressure (P/P$_0$) around 0.0 - 0.2, concaved to the P/P$_0$ axis due to monolayer adsorption in the external surface which were large pores. The lower adsorption volume on 4%K$_2$O/RH-MCM-41 indicated a lower surface area. The adsorption at relative pressure of 0.2 - 0.4 for RH-MCM-41 and 0.4 - 0.8 for K$_2$O/ RH-MCM-41 were adsorptions in the mesopores. The mesopores of 4%K$_2$O/RH-MCM-41 were
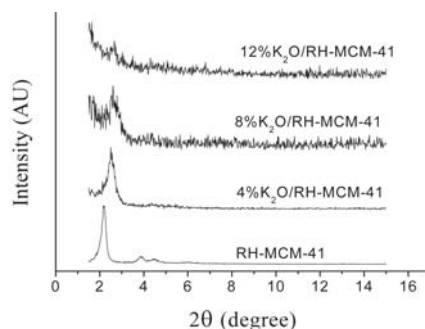
Figure 1. XRD patterns of MCM-41, 4%K$_2$O/ MCM-41, 8%K$_2$O/MCM-41 and 12%K$_2$O/MCM-41

smaller than those in RH-MCM-41, and thus required a higher pressure. The last step was a plateau until the relative pressure approached one and the adsorption volume increased again to form condensation on the surface.

The isotherms of $8\%K_2O/RH$-MCM-41(2c) and $12\%K_2O/RH$-MCM-41(2d) were different from that of $4\%K_2O/RH$-MCM-41, in which the adsorption in mesopores at relative pressure 0.4 - 0.8 disappeared indicating more collapse of the MCM-41 mesoporeous structure. In addition, the adsorption amount at low relative pressure on $8\%K_2O/RH$-MCM-41 and $12\%K_2O/RH$-MCM-41 compared with that on $4\%K_2O/RH$-MCM-41 indicated a lower surface area. These results confirmed the XRD results that the increase of the K_2O content on RH-MCM-41 ruined the mesoporeous structure.

The pore size distributions of the mesopores in RH-MCM-41 and K_2O/RH-MCM-41s were presented in Figure 3. The pore diameter of RH-MCM-41 was centered at 20.4 Å. A small portion of micropores was still present in all K_2O/RH-MCM-41 samples with a diameter of 31.0 Å.

The total pore volume and specific surface area of RH-MCM-41 and K_2O/RH-MCM-41s are presented in Table 2. There was a dramatic decrease of surface area and pore size with the addition of K_2O to RH-MCM-41. In K_2O/RH-MCM-41 samples, the pore size and surface area decreased with the K_2O content. The table also

included the BET results of RH-SiO_2 and 8% $K_2O/$RH-SiO_2. These data were used for comparison in the section below.

Results from Catalytic Testing of K_2O/RH-MCM-41 and K_2O/RH-SiO_2

The conversions of fatty acids are displayed in Figure 4(a-c) in which the formation of methyl palmitate (C16:0), unsaturated methyl esters, including methyl oleate (C18:1), methyl linoleate (C18:2) and methyl linolenate (C18:3), and methyl stearate (C18:0) were plotted versus catalysts with different K_2O loadings, respectively. The formation of methyl esters occurred depending on the amount of fatty acids in the raw material and the most active catalyst for transesterification was $8\%K_2O/RH$-MCM-41. In addition, the conversions over $8\%K_2O/RH$-MCM-41 also depended on temperature. However, the conversions at 100°C were not significantly higher than that at 75°C (namely, 84% versus 82%). As a result, the temperature at 75°C was considered to be the more suitable condition with regard to energy saving.

To compare catalysts on different supports, the catalytic activity of $8\%K_2O/RH$-MCM-41 and that of $8\%K_2O/RH$-SiO_2 were determined at at 100°C and the results are compared in Figure 5. The $8\%K_2O/RH$-MCM-41 gave higher conversion of both C-16 and C-18 than $8\%K_2O/RH$-SiO_2. This might be attributed to the presence of
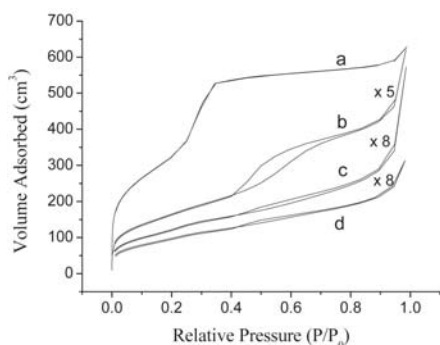

Figure 2. N$_2$ adsorption-desorption isotherm of RH-MCM-41 and K$_2$O/RH-MCM-41; (a) RH-MCM-41 (b) 4%K$_2$O/RH-MCM-41 (c) 8%K$_2$O/RH-MCM-41 (d) 12%K$_2$O/RH-MCM-41
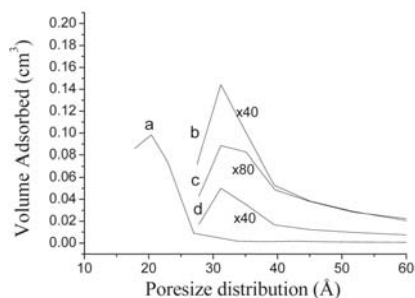
Figure 3. Pore size distribution of RH-MCM-41 and K$_2$O/RH-MCM-41; (a) RH-MCM-41 (b) 4%K$_2$O/RH-MCM-41 (c) 8%K$_2$O/RH-MCM-41 (d) 12% K$_2$O/RH-MCM-41

Table 1. Structure properties data of RH-MCM-41, K$_2$O/RH-MCM-41 and K$_2$O/SiO$_2$

Components	2θ	a* (Å)	d$_{100}$ (Å)
RH-MCM-41	2.3	43.6	37.8
4%K$_2$O/RH-MCM-41	2.5	39.4	34.1
8%K$_2$O/RH-MCM-41	2.6	38.6	33.4
12%K$_2$O/RH-MCM-41	2.7	37.5	32.5

Unit cell parameter of RH-MCM-41 and K$_2$O/RH-MCM-41 of the (100) plane, calculated $a_{100} = \dfrac{2}{\sqrt{3}} d_{100}$

Table 2. Pore volumes and surface areas of RH-SiO$_2$, RH-MCM-41, K$_2$O/RH-SiO$_2$ and K$_2$O/ RH-MCM-41

Components	V$_p$(cm^3/g)*	S$_{BET}$ (m^2/g)
RH-SiO$_2$	0.110	234.20
RH-MCM-41	0.970	1231.40
4%K$_2$O/RH-MCM-41	0.190	118.50
8%K$_2$O/RH-MCM-41	0.110	55.80
8%K$_2$O/RH-SiO$_2$	0.003	6.11
12%K$_2$O/RH-MCM-41	0.060	44.70

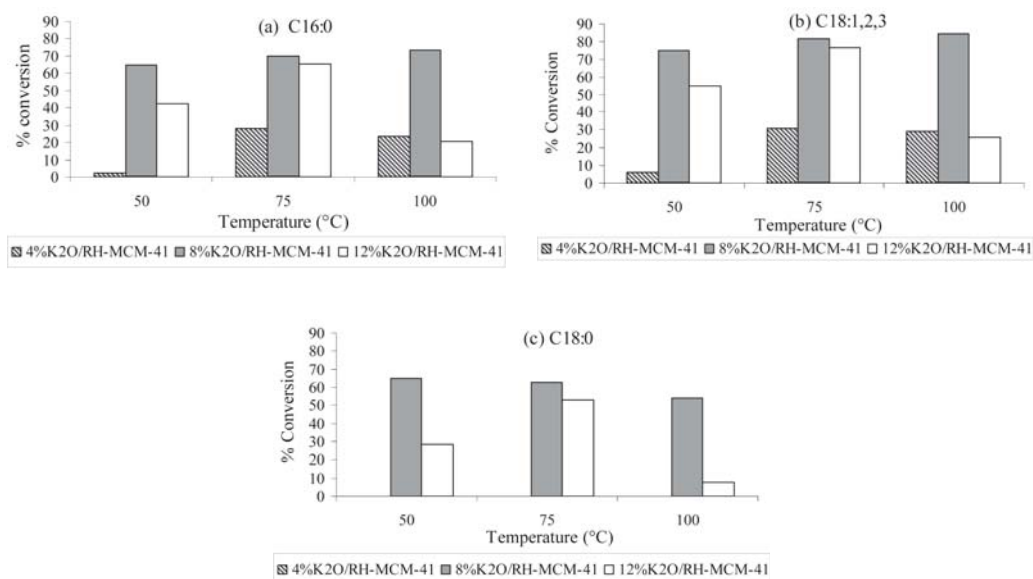* Total pore volumes, calculated from N$_2$ desorption by BJH method.

Figure 4. **(a) Formation of methyl palmitate on K$_2$O/RH-MCM-41 at various temperatures; (b) Formation of unsaturated methyl esters (methyl oleate, C18:1; methyl linoleate, C18:2 and methyl linolenate, C18:3) on K$_2$O/RH-MCM-41 at various temperatures; (c) Formation of methyl stearate (C18:0) on K$_2$O/RH-MCM-41 at various temperatures**

mesoporous structure of the support or difference in the surface areas because the first one still contained mesoporous structure and had a higher surface area (56 versus 6 m^2/g).

Conclusions

Loading K_2O onto RH-MCM-41 significantly changed the support mesoporeous structure resulting in the structure's collapse and a lower surface area. The K_2O/RH-MCM-41 was active for the transesterification of palm olein oil with methanol. The performance depended on the K_2O loading and temperature. The highest conversion was observed on 8%K_2O/RH-MCM-41 at 100°C. Both saturated methyl ester (C16:0) and unsaturated methyl esters (C18:1, C18:2 and C18:3) were obtained with approximately 70 - 80% yield.
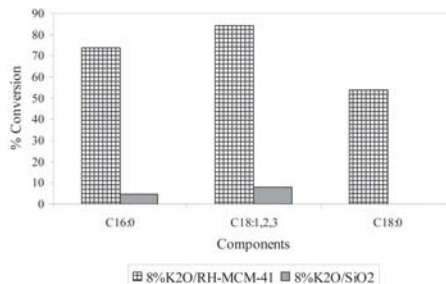
Acknowledgement

Figure 5. Catalytic activity of 8%K_2O supported on RH-MCM-41 and RH-SiO$_2$ at 100°C

References

Kumar, D., Schumacher, K., du Fresne von Hoheneschen, C., GrØn, M., and Unger, K.K. (2001). MCM-41, MCM-48 and related mesoporous adsorbents: their synthesis and characterization. Colloid. Surface. A., 187-188:109-116.

Bialek, R., Meier, W.M., Davis, M., and Annen, M.J. (1991). The synthesis and structure of SSZ-24, the silica analog of AlPO$_4$-5. Zeolites, 11(5):438-422.

Khemthong, P., Prayoonpokarach, S., and Wittayakun, J. (2007). Synthesis and characterization of zeolite LSX from rice husk silica. Suranaree J. Sci. Technol., 12(4):367-379.

Grisdanurak, N., Chiarakorn, S. and Wittayakun, J. (2003). Utilization of mesoporous molecular sieves synthesized from natural source rice husk silica to chlorinated volatile organic compounds (CVOC) adsorption. Korean J. Chem. Eng., 20(5):950-955.

Ma, F. and Hanna, M.A. (1999). Biodiesel production: a review. Bioresour. Technol., 70(1):1-15.

Srinivas, D., Srivastava, R., and Ratnasamy, P. (2004). Transesterifications over titanosilicate molecular sieves. Catal. Today, 96(3):127-133.

Xie, W., Huang, X., and Li, H. (2006). Soybean oil methyl ester preparation using NaX Zeolite loaded with KOH as a heterogeneous catalyst. Bioresour. Technol., 98(4):936-939.

Park, S-H., Kim, B-H., Selvaraj, M., and Lee,T-G. (2007). Synthesis and characterization of mesoporous Ce-Mn-MCM-41 molecular sieves. J. Ind. Eng. Chem., 13(4):637-643.

Papp, A., Molnár, Á., and Mastalir, Á. (2005). Catalytic investigation of Pd particles supported on MCM-41 for the selective hydrogenations of terminal and internal alkynes. Appl. Catal. A-Gen., 289(2):256-266.

Department of Agriculture, Suratthani Oil Palm Research Center. (2007). Available from: http://www.doa.go.th/palm/linkTechnical/processOilpalm.html. Accessed date: Dec 11, 2007.